Computation over Wide-Band Multi-Access Channels: Achievable Rates Through Sub-Function Allocation

Fangzhou Wu, Li Chen, Nan Zhao, *Senior Member, IEEE,* Yunfei Chen, *Senior Member, IEEE,* F. Richard Yu, *Fellow, IEEE,* and Guo Wei

***Abstract*—Future networks are expected to connect an enormous number of nodes wirelessly using wide-band transmission. This brings great challenges. To avoid collecting a large amount of data from the massive number of nodes, computation over multi-access channel (CoMAC) is proposed to compute a desired function over the air utilizing the signal-superposition property of wireless channel. Due to frequency-selective fading, wide-band CoMAC is more challenging and has never been studied before. In this work, we propose the use of orthogonal frequency division multiplexing (OFDM) in wide-band CoMAC to transmit functions in a similar way to bit sequences through division, allocation, and reconstruction of functions. An achievable rate without any adaptive resource allocation is derived. To prevent a vanishing computation rate from the increase in the number of nodes, a novel sub-function allocation of sub-carriers is derived. Furthermore, we formulate an optimization problem considering power allocation. A sponge-squeezing algorithm adapted from the classical water-filling algorithm is proposed to solve the optimal power allocation problem. The improved computation rate of the proposed framework and the corresponding allocation has been verified through both theoretical analysis and simulation.**

***Index Terms*—Achievable computation rate, OFDM, optimal power allocation, sub-function allocation, wide-band transmission, wireless networks.**

I. Introduction

CURRENT 5G and the Internet of Things envision the interconnections of up to 1 trillion products, machines and devices through wide-band transmission [1]–[3]. With such an enormous number of nodes, it is impractical to transmit data using conventional orthogonal multi-access schemes in future networks because this would result in excessive network latency and low spectrum utilization efficiency.

To solve this problem, computation over multi-access channel (CoMAC) was proposed to exploit the signal-superposition property of multi-access channel (MAC) to compute the desired function through concurrent node transmissions, which combines computation with communication [4]–[19]. A straightforward application of CoMAC to attain transmission and computation in parallel is wireless sensor networks, whose communication goal is typically for a fusion center to obtain a function value of the sensor readings (e.g., arithmetic mean, polynomial or number of active nodes), rather than to store all readings from all sensors. Otherwise, CoMAC can also be applied in networks that focus on computing a class of so called nomographic functions of distributed data via concurrent node transmissions [4].

A simple computation framework, called analog CoMAC, has been studied in [5]–[10]. In analog CoMAC, all nodes participate in the transmission. The authors used pre-processing at each node and post-processing at the fusion center to deal with channel fading and compute functions [5]. The designs of pre-processing and post-processing used to compute linear and non-linear functions have been discussed in [6], and the effect of channel estimation error was characterized in [7]. In order to verify whether analog CoMAC is feasible in practice, an implementation using software defined radio was built in [8]. A multi-function computation method utilizing a multi-antenna fusion center to collect data transmitted by a cluster of multi-antenna multi-modal sensors has been presented in [9]. Furthermore, using multiplexing gain to compute multiple functions has been discussed in [10]. In summary, simple analog CoMAC has led to an active area focusing on the design and implementation techniques for receiving a desired function of concurrent signals.

The main limitation of analog CoMAC is the lack of robust design against noise. Hence, digital CoMAC using joint source-channel coding in [11]–[19] was proposed to reduce the noise effect. The potential of linear source coding was discussed in [11], and its application was presented in [12] for the function computation over MAC. Compared with linear source coding, nested lattice coding can approach the performance of standard random coding [13]. This lattice-based CoMAC was extended to a general framework in [15] for relay networks with linear channels and additive white Gaussian noise. In order to combat non-uniform fad-

This research was supported by National Natural Science Foundation of China (Grant No. 61601432), the Fundamental Research Funds for the Central Universities, and the open research fund of National Mobile Communications Research Laboratory, Southeast University (No. 2018D03). This paper was presented in part at the IEEE Wireless Communications and Networking Conference (WCNC), Marrakech, Morocco, April 2019.(*Corresponding author: Li Chen*)

F. Wu, L. Chen and G. Wei are with Department of Electronic Engineering and Information Science, CAS Key Laboratory of Wireless-Optical Communications, University of Science and Technology of China, Hefei, Anhui 230027. (e-mail: fangzhouwu@outlook.com, {chenli87, wei}@ustc.edu.cn).

N. Zhao is with the School of Information and Communication Engineering, Dalian University of Technology, Dalian 116024, China, and also with the National Mobile Communications Research Laboratory, Southeast University, Nanjing 210096, China (e-mail: zhaonan@dlut.edu.cn).

Y. Chen is with the School of Engineering, University of Warwick, Coventry CV4 7AL, U.K. (e-mail: Yunfei.Chen@warwick.ac.uk).

F.R. Yu is with the Department of Systems and Computer Engineering, Carleton University, Ottawa, ON, K1S 5B6, Canada. (email: richard.yu@carleton.ca).

ing, a uniform-forcing transceiver design was given in [14]. Achievable computation rates were given in [15]–[17] for digital CoMAC through theoretical analysis. In [17], Jeon and Bang found that the computation rates achieved by the above computation techniques decrease as the number of nodes increases, and eventually go to zero due to fading MAC. To handle this problem, they proposed an opportunistic CoMAC where a subset of the nodes opportunistically participated in the transmission at each time, which provided a non-vanishing computation rate even when the number of nodes in the network goes to infinity.

To the best of our knowledge, the above mentioned works only consider CoMAC with single-carrier flat fading. A wide-band CoMAC has not been discussed before and needs to be extended. Wide-band signal transmission has to endure frequency-selective fading because the coherence bandwidth of the channel is always smaller than the signal bandwidth. In the time domain, the multi-path interference is not easy to be removed [20]. Orthogonal frequency division multiplexing (OFDM) is an effective solution to inter-symbol interference caused by the dispersive channel [21]–[23], and has been applied in many communication fields. Also, the orthogonal channels of OFDM in the frequency domain is equivalent to a chief executive officer (CEO) problem where the decoder is interested in reconstructing the symbols in each sub-carrier [24]–[26]. The CEO problem is relevant for studying the general multi-terminal problem, which is foundational and has great potential. In [25], the authors have studied the rate-distortion region of the discrete memoryless multi-encoder CEO problem. As for the vector Gaussian CEO problem, a complete characterization of the rate-distortion region of it under logarithmic loss distortion measure has been presented by [26]. For a more practical application, the authors in [27] established and utilized the connections between cloud radio access networks and the CEO source coding problem under logarithmic loss distortion measure to analyze the capacity of the radio access network.

Motivated by the above observations, we employ OFDM in the implementation of CoMAC. However, the conventional OFDM systems which load bit sequences of different lengths into different sub-carriers cannot be used directly because CoMAC transmits a desired function over the air, not a bit sequence. Thus, the desired function as a whole cannot be allocated into several sub-carriers. To deal with this issue, we propose a method of sub-function allocation for the division, allocation, and reconstruction of the desired function. This method divides the desired function into some sub-functions, allocates these sub-functions into different sub-carriers, and reconstructs the desired function at the fusion center. The theoretical expression of the achievable computation rate is derived based on the classical results of nested lattice coding [16]–[19]. It is shown to provide a non-vanishing computation rate as the number of nodes increases. An optimization problem considering power allocation is further discussed, and a sponge-squeezing algorithm adapted from the classical water-filling algorithm is proposed to solve the optimal power allocation problem. Owing to sub-function allocation and power allocation, the computation rate is significantly improved. Our

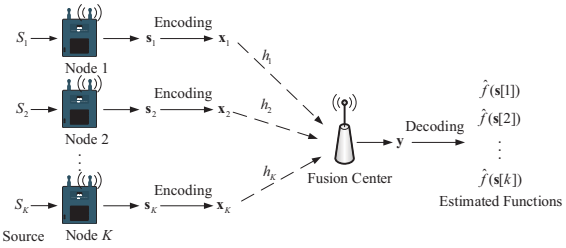

Fig. 1. A classical framework of CoMAC.

contributions can be summarized as follows:

- *Novel CoMAC-OFDM*. In order to tackle frequency-selective fading, we exploit the mechanism of OFDM to implement wide-band CoMAC. Unlike the conventional CoMAC schemes, CoMAC-OFDM divides a desired function into sub-functions, allocates sub-functions to each sub-carrier and reconstructs the desired function at the fusion center.
- *Improved computation rate*. A novel sub-function allocation is designed to assign sub-functions to sub-carriers, which provides a non-vanishing computation rate as the number of nodes increases. After that, the theoretical expression of improved computation rate is derived.
- *Optimal power allocation*. An optimal power allocation is considered to improve computation rate. Since the solution of our optimization is not suitable to utilize the classical water-filling algorithm, we propose a sponge-squeezing algorithm adapted from the classical water-filling algorithm to carry out the power allocation, which provides a simple and concise interpretation of the necessary optimality conditions.

The paper is organized as follows. Section II introduces the definitions of CoMAC and the system model for CoMAC-OFDM. In Section III, we summarize the main results of this paper and compare them with existing results. Section IV presents the proposed CoMAC-OFDM with sub-function allocation in detail and analyzes the computation rate. Section V focuses on the improvement of the computation rate using power allocation. Simulation results are presented in Section VI and conclusions are given in Section VII.

II. Preliminaries & Network Model

In this section, we give some definitions before introducing CoMAC. Throughout this paper, we denote $[1:n] = \{1, 2, \cdots, n\}$, and $\mathsf{C}^+(x) = \max\left\{\frac{1}{2}\log(x), 0\right\}$. For a set $\mathcal{A}$, $|\mathcal{A}|$ denotes the cardinality of $\mathcal{A}$. $\lceil x \rceil$ is the ceiling function as $\lceil x \rceil = \min\{n \in \mathbb{Z} | x \leq n\}$. Let the entropy of a random variable A be $H(A)$ and $\mathrm{diag}\{a_1, a_2, \cdots, a_n\}$ denote the diagonal matrix of which the diagonal elements are from a_1 to a_n. A set $\{x_1, x_2, \cdots, x_N\}$ is written as $\{x_i\}_{i\in[1:N]}$ for short. $(\cdot)^{\mathrm{T}}$ represents the transpose of a vector or matrix. A vector is regarded as a row vector in this paper.

A. CoMAC

A classical framework of CoMAC is depicted in Fig. 1. In this framework, the fusion center is designed to compute a desired function from K nodes. Each node obtains data from a corresponding random source for T_d times, and then provides a data vector of length T_d.

Definition 1 (Data Matrix): Assume that S_i is a random source from which the i-th node gets data, and let $\mathbf{b_v} = [S_1, S_2, \cdots, S_K]$ be a random vector associated with a joint probability mass function $p_{\mathbf{b_v}}(\cdot)$. A data matrix $\mathbf{S} \in \mathbb{C}^{K\times T_d}$ represents the data from K nodes during T_d time slots. It is expressed as

$$\begin{aligned}\mathbf{S} &= \begin{bmatrix} s_1[1] & \cdots & s_1[j] & \cdots & s_1[T_d] \\ \vdots & \ddots & \vdots & \ddots & \vdots \\ s_i[1] & \cdots & s_i[j] & \cdots & s_i[T_d] \\ \vdots & \ddots & \vdots & \ddots & \vdots \\ s_K[1] & \cdots & s_K[j] & \cdots & s_K[T_d] \end{bmatrix} \\ &= \begin{bmatrix} \mathbf{s}[1]^{\mathrm{T}} & \cdots & \mathbf{s}[j]^{\mathrm{T}} & \cdots & \mathbf{s}[T_d]^{\mathrm{T}} \end{bmatrix} \\ &= \begin{bmatrix} \mathbf{s}_1^{\mathrm{T}} & \cdots & \mathbf{s}_i^{\mathrm{T}} & \cdots & \mathbf{s}_K^{\mathrm{T}} \end{bmatrix}^{\mathrm{T}}, \end{aligned} \tag{1}$$

where $j \in [1 : T_d]$, $i \in [1 : K]$, $s_i[j]$ is the j-th data of the i-th node from the random source S_i, $\mathbf{s}[j] = [s_1[j], \cdots, s_K[j]]$ is the j-th data of all K nodes and $\mathbf{s}_i = [s_i[1], \cdots, s_i[T_d]]$ is the data vector of node i. Note that $s_i[j]$ belongs to $[0 : p-1]$, which means it is mapped to a number between 0 and $p-1$ through quantization. Also, $\mathbf{s}[j]$ is independently drawn from $p_{\mathbf{b_v}}(\cdot)$.

Using Definition 1, the desired function determined by the random source vector $\mathbf{b_v}$ can be expressed as $f(\mathbf{b_v})$, and its definition is given as follows.

Definition 2 (Desired Function): For all $j \in [1 : T_d]$, every function

$$f(s_1[j], s_2[j], \cdots, s_K[j]) = f(\mathbf{s}[j]) \tag{2}$$

that has to be computed at the fusion center is called a desired function where $\mathbf{s}[j]$ is independently drawn from $p_{\mathbf{b_v}}(\cdot)$ (see Definition 1). Every function $f(\mathbf{s}[j])$ can be seen as a realization of $f(\mathbf{b_v})$. Thus, it has T_d functions where each node gets data from each random source for T_d times.

Remark 1: As studied in [16], [18], [19], [28], CoMAC is designed to compute different types of desired functions. There are two typical functions that we focus on. A function $f(\mathbf{s}[j])$ whose values are in the set $\{\sum_{i=1}^{K} a_{1,i}s_i[j], \cdots, \sum_{i=1}^{K} a_{L_s,i}s_i[j]\}$ is called the arithmetic sum function, where $a_{l,i} \in \mathbb{R}$ is the weighting factor for node i, and L_s belongs to $\mathbb{N}$. The arithmetic sum function is a weighted sum function, which includes the mean function for all K nodes $f(\mathbf{s}[j]) = \frac{1}{K}\sum_{i=1}^{K} s_i[j]$ and the function for the active node only $f(\mathbf{s}[j]) = \{s_1[j], s_2[j], \cdots, s_K[j]\}$ as special cases. Apart from this, a function $f(\mathbf{s}[j])$ with values in the set of $\{\sum_{i=1}^{K} \mathbf{1}_{s_i[j]=0}, \cdots, \sum_{i=1}^{K} \mathbf{1}_{s_i[j]=p}\}$ is regarded as the type function where $\mathbf{1}_{(\cdot)}$ denotes the indicator function. As pointed out in [28], any symmetric function such as mean, variance, maximum, minimum and median can be attained from the type function.

Definition 2 shows that the desired function $f(\mathbf{s}[j])$ is computed by all K nodes participating in the computation. In some cases, we only need to choose M nodes to participate in the computation each time. Then the desired function $f(\mathbf{s}[j])$ has to be divided into $B = \frac{K}{M} \in \mathbb{N}$ parts. A function that only uses some of the nodes is called a sub-function, and its definition is given as follows.

Definition 3 (Sub-Function): Let

$$\tau_u = \{x \in [1 : K] : |\tau_u| = M\} \tag{3}$$

denote a set where each element x is an index from the M chosen nodes. Supposing that $\bigcup_{u=1}^{B} \tau_u = [1 : K]$ and $\tau_u \bigcap \tau_v = \emptyset$ for all $u, v \in [1 : B]$, a function $f\left(\{s_i[j]\}_{i\in\tau_u}\right)$ is said to be a sub-function if and only if there exists a function $f_c(\cdot)$ satisfying $f(\mathbf{s}[j]) = f_c\left(f\left(\{s_i[j]\}_{i\in\tau_1}\right), f\left(\{s_i[j]\}_{i\in\tau_2}\right), \cdots, f\left(\{s_i[j]\}_{i\in\tau_B}\right)\right)$.

Thus, the fusion center reconstructs the desired function based on B sub-functions, when K nodes are divided into B parts.

In order to achieve reliable computations against noise, we apply block codes named sequences of nested lattice codes [15] throughout this paper. Based on the block coding, the definitions of encoding and decoding are given as follows.

Definition 4 (Encoding & Decoding): For the i-th node, let $\mathbf{s}_i$ denote the data vector whose length is T_d (see Definition 1). Denote $\mathbf{x}_i = [x_i[1], x_i[2], \cdots, x_i[n]]$ as the length-n transmitted vector for node i. The length-n received vector is given by $\mathbf{y} = [y[1], y[2], \cdots, y[n]]$ at the fusion center. Assuming there is a block code with length $n \geq T_d$, the encoding and decoding functions can be expressed as follows.

- *Encoding Functions*: the univariate function $\boldsymbol{\mathcal{E}}_i(\cdot)$ which generates $\mathbf{x}_i = \boldsymbol{\mathcal{E}}_i(\mathbf{s}_i)$ is an encoding function of node i. This means that $\mathbf{s}_i$ of length T_d is mapped to a transmitted vector $\mathbf{x}_i$ of length n for node i.
- *Decoding Functions*: the decoding function $\boldsymbol{\mathcal{D}}_j(\cdot)$ is used to estimate the j-th desired function $f(\mathbf{s}[j])$, which satisfies $\hat{f}(\mathbf{s}[j]) = \boldsymbol{\mathcal{D}}_j(\mathbf{y})$. This implies that the fusion center obtains T_d desired functions depending on the whole received vector of length n.

Considering a block code of length n, the definition of computation rate [4], [16], [17], [19] can be given as follows.

Definition 5 (Computation Rate): The computation rate specifies how many function values can be computed per channel use within a predefined accuracy. It can be written as $R = \lim_{n\to\infty} \frac{T_d}{n} H(f(\mathbf{b_v}))$, where T_d is the number of function values (see Definition 2), n is the length of the block code and $H(f(\mathbf{b_v}))$ is the entropy of $f(\mathbf{b_v})$. R is achievable only if there is a length-n block code such that the probability $\Pr\left(\bigcup_{j=1}^{T_d}\left\{\hat{f}(\mathbf{s}[j] \neq f(\mathbf{s}[j]))\right\}\right) \to 0$ as n increases.

B. Fading MAC with Wide-band signal

Wide-band signal transmission has to endure frequency-selective fading because the coherence bandwidth of the channel is smaller than the signal bandwidth. OFDM is well-suited to provide robustness against fading. Thus, we describe a CoMAC-OFDM system with N sub-carriers during T_s OFDM

symbols, and the length of the block code is n. Then, the m-th received OFDM symbol at the fusion center in the frequency domain can be given as

$$\boldsymbol{Y}[m] = \sum_{i=1}^{K} \boldsymbol{V}_i[m]\boldsymbol{X}_i[m]\boldsymbol{H}_i[m] + \boldsymbol{W}[m], \tag{4}$$

where $T_s = \lceil \frac{n}{N} \rceil$, $\boldsymbol{V}_i[m] = \operatorname{diag}\left\{ \frac{|h_{i,1}[m]|}{h_{i,1}[m]}\sqrt{P_{i,1}[m]}, \cdots, \frac{|h_{i,N}[m]|}{h_{i,N}[m]}\sqrt{P_{i,N}[m]} \right\}$ is the power allocation matrix of node i where each diagonal element $\frac{|h_{i,g}[m]|}{h_{i,g}[m]}\sqrt{P_{i,g}[m]}$ is the power allocated to the g-th sub-carrier, $\boldsymbol{H}_i[m] = \operatorname{diag}\{h_{i,1}[m], \cdots h_{i,N}[m]\}$ is a diagonal matrix of which the diagonal element is the frequency response of each sub-carrier for node i, the transmitted diagonal matrix of node i at the m-th OFDM symbol is $\boldsymbol{X}_i[m] = \operatorname{diag}\{x_{i,1}[m], x_{i,2}[m], \cdots, x_{i,N}[m]\}$, the diagonal element $x_{i,g}[m]$ in $\boldsymbol{X}_i[m]$ represents an element whose index is $(m-1)N+g$ in the transmitted vector $\mathbf{x}_i$ (see Definition 4) for node i and the diagonal element of $\boldsymbol{W}[m]$ can be regarded as identically and independently distributed (i.i.d.) complex Gaussian random noise following $\mathcal{CN}(0,1)$.

According to the above expression, the received signal in the g-th sub-carrier at the m-th OFDM symbol can be expressed as

$$y_g[m] = \sum_{i=1}^{K} x_{i,g}[m]v_{i,g}[m]h_{i,g}[m] + w_{i,g}[m], \tag{5}$$

where $g \in [1:N]$, $m \in [1:T_s]$, $v_{i,g}[m]$ is the g-th diagonal element from $\boldsymbol{V}_i[m]$, $h_{i,g}[m]$ from $\boldsymbol{H}_i[m]$ is the frequency response of the g-th sub-carrier of node i at the m-th OFDM symbol and $w_{i,g}[m]$ is i.i.d. complex Gaussian random noise following $\mathcal{CN}(0,1)$.

The above equations assume perfect synchronization and perfect removal of inter-carrier interference.

III. Problem Statement & Main Results

In this section, we first introduce several existing CoMAC schemes with their features and limitations. Then, we describe our main results and present their improvements compared with these existing CoMAC schemes. For easy presentation in following sections, we define the ordered indexes to describe the indexes of nodes that are sorted by the corresponding channel gain. For the g-th sub-carrier, let $\mathcal{I}_i^g \in [1:K]$ be the i-th element in the set of ordered indexes of $[1:K]$ such that $|h_{\mathcal{I}_1^g}| \geq |h_{\mathcal{I}_2^g}| \geq \cdots \geq |h_{\mathcal{I}_K^g}|$, e.g., $\min_{i\in[1:K]}|h_{i,g}|^2 = |h_{\mathcal{I}_K^g}|^2$. Furthermore, g can be omitted if the number of sub-carriers N is 1.

A. Previous Works

In [16], the authors provided the computation rate for the arithmetic sum and type functions (see Remark 1) in fading MAC, i.e., the channel coefficients are i.i.d. and vary independently over time. The rate of CoMAC based on single carrier (CoMAC-SC) considering flat fading is shown as follows.

Theorem 1 (Direct CoMAC-SC Rate): Based on [16, Theorem 3], the computation rate with an average power constraint in each time slot is given as

$$\begin{aligned} R =& \mathsf{E}\left[\mathsf{C}^+\left(\frac{1}{K} + \frac{\min_{i\in[1:K]}\left[|h_i|^2 P\right]}{\mathsf{E}\left[\frac{\min_{i\in[1:K]}|h_i|^2}{|h|^2}\right]} \right)\right] \\ \overset{(a)}{=}& \mathsf{E}\left[\mathsf{C}^+\left(\frac{1}{K} + \frac{|h_{\mathcal{I}_K}|^2 P}{\mathsf{E}\left[\frac{|h_{\mathcal{I}_K}|^2}{|h|^2}\right]} \right)\right], \end{aligned} \tag{6}$$

where $\frac{1}{\mathsf{E}\left[|h_{\mathcal{I}_K}|^2/|h|^2\right]} \geq 1$ is the gain from the average power constraint, each channel response of the i-th node h_i and the representative coefficient h without loss of generality are i.i.d. random variables and the condition (a) follows based on the ordered indexes.

Unfortunately, for wireless networks with a massive number of nodes, the computation rate approaches 0 as K increases, which is a vanishing computation rate. To resolve the problem, an opportunistic CoMAC-SC system has been discussed in [17]. In each time slot, only M nodes with the M largest channel gains participate in the transmission such that the indexes of the M chosen nodes is in the set $\{\mathcal{I}_i\}_{i\in[1:M]}$.

Theorem 2 (Opportunistic CoMAC-SC Rate): As shown in [17, Theorem 1], for any $M, B \in \mathbb{N}$ satisfying $MB = K$, the computation rate of the opportunistic CoMAC-SC with average power constraint is given by

$$R = \frac{1}{B}\mathsf{E}\left[\mathsf{C}^+\left(\frac{1}{M} + \frac{|h_{\mathcal{I}_M}|^2 KP}{M\mathsf{E}\left[\frac{|h_{\mathcal{I}_M}|^2}{|h|^2}\right]} \right)\right], \tag{7}$$

where $\mathcal{I}_M$ is the M-th element of the set of ordered indexes $\{\mathcal{I}_i\}_{i\in[1:K]}$.

Theorem 2 shows an improved computation rate in fading environments and provides a non-vanishing computation rate as K increases. However, wide-band CoMAC with frequency-selective fading has not been discussed, and the improvement of computation rate is still limited in [4], [12], [16]–[19], [28]–[30]. Therefore, our paper focuses on designing a framework of CoMAC for wide-band transmission, which can be robust against both frequency-selective fading and the vanishing computation rate. Then, under our sub-function allocation and power allocation, we compare our scheme to these CoMAC-SC schemes considered in [16], [17]. The results show that our scheme achieves a higher computation rate and also provides a non-vanishing computation rate.

B. Main Results

We employ OFDM design into wide-band CoMAC and divide a desired function into $B = \frac{K}{M} \in \mathbb{N}$ sub-functions. By allocating these sub-functions to different sub-carriers, the computation rate based on CoMAC-OFDM is presented in Theorem 3.

Theorem 3 (General CoMAC-OFDM Rate): For any $M, N \in \mathbb{N}$ satisfying $M \leq K$, the computation rate of wide-band CoMAC-OFDM over fading MAC is given by

$$R = \frac{M}{KN}\frac{1}{T_s}\sum_{m=1}^{T_s}\left[\sum_{g=1}^{N}\mathsf{C}^+\left(\frac{N}{M} + N\times \min_{i\in[1:M]}\left[|h_{\mathcal{I}_i^g}[m]|^2 P_{\mathcal{I}_i^g}[m]\right]\right)\right] \quad (8)$$

$$\overset{(a)}{=} \frac{M}{KN}\mathsf{E}\left[\sum_{g=1}^{N}\mathsf{C}^+\left(\frac{N}{M} + N\min_{i\in[1:M]}\left[|h_{\mathcal{I}_i^g}|^2 P_{\mathcal{I}_i^g}\right]\right)\right], \quad (9)$$

where the condition (a) follows as $T_s \to \infty$, T_s is the number of OFDM symbols as shown in Eqs. (4) and (5), K is the number of nodes for a desired function (see Definition 2), M is the number of the chosen nodes for a sub-function (see Definition 3), N is the number of the sub-carriers for each OFDM symbol, $h_{\mathcal{I}_i^g}[m]$ is the frequency response of the g-th sub-carrier of node $\mathcal{I}_i^g[m]$, $P_{\mathcal{I}_i^g}[m]$ is the power allocated to the $\mathcal{I}_i^g[m]$-th node in the g-th sub-carrier at the m-th OFDM symbol and $\mathcal{I}_i^g[m]$ is the i-th element of the ordered indexes in the g-th sub-carrier at the m-th OFDM symbol.

Proof: We refer to Section IV for proof. ■

Remark 2: The rate in Theorem 3 is given as a general computation rate for wide-band CoMAC-OFDM, and the achievable rate for any power allocation method can be derived through Theorem 3. It also generalizes the results for CoMAC-SC schemes in Theorems 1 and 2 by setting the number of sub-carriers N to 1.

A simple computation rate for wide-band CoMAC-OFDM system without sub-function allocation and adaptive power allocation can be easily obtained from Theorem 3.

Corollary 1 (Direct CoMAC-OFDM Rate): For a straightforward wide-band CoMAC-OFDM system, each desired function is assigned to each sub-carrier directly, and the node i has an identical average power constraint in the g-th sub-carrier, i.e., $\mathsf{E}\left[|x_{i,g}[m]|^2\right] \leq \frac{P}{N}$ for all $i \in [1:K]$ and $g \in [1:N]$. The computation rate can be given as

$$R_{C1} = \mathsf{E}\left[\mathsf{C}^+\left(\frac{N}{K} + \frac{|h_{\mathcal{I}_K}|^2 P}{\mathsf{E}\left[\frac{|h_{\mathcal{I}_K}|^2}{|h|^2}\right]}\right)\right]. \quad (10)$$

Proof: We refer to Section V-A for proof. ■

By setting $N = 1$ in Corollary 1, the rate of direct CoMAC-OFDM is the same as the rate of direct CoMAC-SC in Theorem 1. By comparing (6) and (10), the computation rate of direct CoMAC-OFDM can be improved as the number of sub-carriers N increases. However, even though N can keep increasing, it still has an upper limit and cannot be infinity in practice. Thus, the computation rates in Eqs. (6) and (10) would become vanishing as the number of nodes K increases and converge to 0 in fading MAC.

In order to deal with this, we propose sub-function allocation to avoid the vanishing computation rate even if the number of nodes K in the network increases. Based on Theorem 3, the computation rate of CoMAC-OFDM with sub-function allocation can be expressed as follows.

Corollary 2 (CoMAC-OFDM Rate With Sub-Function Allocation and Average Power Allocation): Suppose that a desired function is divided into B sub-functions, and each sub-function is allocated to a sub-carrier where the channel gains of the M nodes are the largest. The computation rate of wide-band CoMAC-OFDM with sub-function allocation and average power allocation can be given as

$$R_{C2} = \frac{M}{K}\mathsf{E}\left[\mathsf{C}^+\left(\frac{N}{M} + \frac{|h_{\mathcal{I}_M}|^2 KP}{M\mathsf{E}\left[\frac{|h_{\mathcal{I}_M}|^2}{|h|^2}\right]}\right)\right]. \quad (11)$$

Proof: We refer to Section V-A for proof. ■

By setting $N = 1, K = MB$ in Corollary 2, the computation rate is the same as that in Theorem 2. Compared with Eq. (7), it shows that the proposed scheme can not only provide a non-vanishing computation rate but also improve the computation rate when the number of sub-carriers N increases.

In addition to average power allocation, OFDM can achieve a higher rate with adaptive power allocation for each node. The instantaneous computation rate for a OFDM symbol is obtained as follows.

Corollary 3 (CoMAC-OFDM Rate With Sub-Function Allocation and Optimal Power Allocation): The optimal computation rate with sub-function allocation at the m-th OFDM symbol is given as

$$R_{C3}[m] = \frac{M}{KN}\sum_{g=1}^{N}\mathsf{C}^+\left(\frac{N}{M} + N\eta_g^*[m]\right), \quad (12)$$

where $\eta_g^*[m]$ is the optimal level for the g-th sub-carrier at the m-th OFDM symbol, which will be further explained in Section V-B .

Proof: We refer to Section V-B1 for the proof. ■

Depending on the proposed sub-function allocation, we consider an optimization problem to achieve a higher computation rate in OFDM with a total power constraint for each node. Based on the solution to the optimization problem, we propose a sponge-squeezing algorithm to implement the optimal power allocation method.

IV. Sub-Function Allocation for CoMAC-OFDM

In this section, we explain the framework of CoMAC-OFDM, which is designed to transmit wide-band signals and improve the computation rate. In Section IV-A, we present sub-function allocation and expound some technical issues that need to be addressed. Then, we resolve these issues and provide the computation rate in Sections IV-B and Section IV-C.

A. Sub-Function Allocation

As shown in Fig. 2, sub-function allocation includes three main parts: function division, function allocation, and function reconstruction. We provide a simplified description of sub-function allocation based on the CoMAC-OFDM system as follows.

- *Function Division.* In Fig. 2a, Node i gets data from the corresponding random source and obtains the data

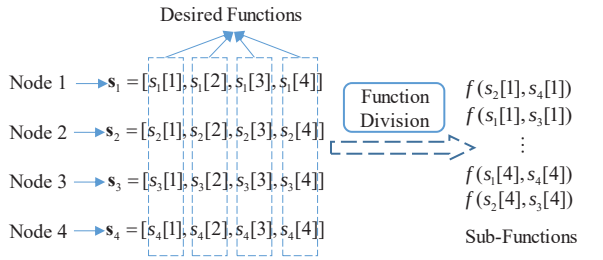

(a) Function division

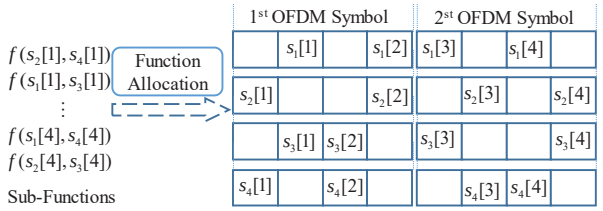

(b) Function allocation

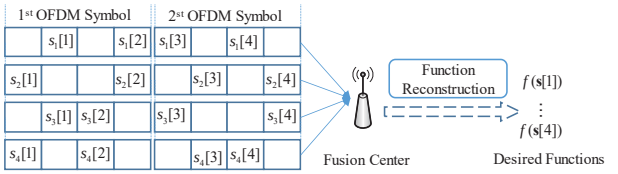

(c) Function reconstruction

Fig. 2. Implementation of sub-function allocation through division, allocation and reconstruction of function in CoMAC-OFDM.

vector $\mathbf{s}_i$. Then, 4 desired functions are divided into 8 sub-functions, which means that only 2 chosen nodes participate in the computation for a given sub-function.

- *Function Allocation.* Each sub-function is only allocated to the sub-carrier where the channel gains of the chosen nodes are the largest. For a sub-function $f(s_1[4], s_4[4])$ in Fig. 2b, the chosen nodes are Node 1 and Node 4. When the channel gains of Nodes 1 and 4 are the largest ones in the third sub-carrier at the second OFDM symbol, e.g., $|h_1| \geq |h_4| \geq |h_2| \geq |h_3|$, the sub-function $f(s_1[4], s_4[4])$ should be assigned to this sub-carrier. After function allocation, all the nodes transmit the corresponding OFDM symbols over the air.
- *Function Reconstruction.* In Fig. 2c, two OFDM symbols are received at the fusion center, and each sub-function can be obtained in each sub-carrier. Then, 4 desired functions can be reconstructed using 8 received sub-functions.

However, the above description of sub-function allocation is ideal, and the following practical issues should be addressed.

i. The order of the channel gains at each sub-carrier is random and depends on the channel realizations in practice. This means that rules for sub-function allocation should be established.
ii. The above description ignores the encoding and decoding of the nested lattice code. How to employ sequences of nested lattice codes in sub-function allocation needs to be addressed.

Further discussion on solving these issues is in Section IV-C.

B. Computation Rate for Sub-Functions

As shown in Section IV-A, the fusion center computes one sub-function at a sub-carrier. Each sub-function is only allocated to the sub-carrier where the channel gains of the chosen M nodes are the M largest ones. The indexes of those chosen nodes are in a set $\{\mathcal{I}_i^g[m]\}_{i=1}^M$ for the g-th sub-carrier at the m-th OFDM symbol. For the sake of fairness, we assume the bandwidth of CoMAC-OFDM with N sub-carriers is the same as the bandwidth of CoMAC-SC. Thus, the bandwidth of the sub-carrier is $\frac{1}{N}$ of the total bandwidth, and the noise power in a sub-carrier scales down with the number of sub-carriers N. Then, the computation rate of a sub-function at the m-th OFDM symbol can be given as follows.

Lemma 1: As the length of block code $n \to \infty$, the instantaneous computation rate of a single sub-function in the g-th sub-carrier at the m-th OFDM symbol with additive white Gaussian noise and unit variance is given as

$$R_{\rho,g}[m] = \frac{1}{N}\mathsf{C}^+\left(\frac{N}{M} + N \min_{i\in[1:M]}\left[|h_{\mathcal{I}_i^g}[m]|^2 P_{\mathcal{I}_i^g}[m]\right]\right), \tag{13}$$

where $h_{\mathcal{I}_i^g}[m]$ is the frequency response of the g-th sub-carrier for node $\mathcal{I}_i^g[m]$ (see Eq. (5)) and $P_{\mathcal{I}_i^g}[m]$ is the allocated power of the $\mathcal{I}_i^g[m]$-th node in the g-th sub-carrier at the m-th OFDM symbol.

Proof: [15, Theorem 4 and Eq. (85)] shows that the computation rate with a noise power of σ_Z^2 and the symbol power of P is given as

$$R = \mathsf{C}^+\left(\frac{1}{\sigma_Z^2}\left(\|\boldsymbol{a}\|^2 - \frac{P\left|\boldsymbol{h}^H\boldsymbol{a}\right|^2}{1+P\|\boldsymbol{h}\|^2}\right)^{-1}\right), \tag{14}$$

where $\boldsymbol{a}$ is the equation coefficient vector and $\boldsymbol{h}$ is the channel coefficient vector with ± 1 entries.

By setting $\sigma_Z^2 = \frac{1}{N}, \boldsymbol{a} = \boldsymbol{h}$ and using [15, Theorems 4 and 11], the computation rate can be written as

$$R = \mathsf{C}^+\left(\frac{N}{M} + NP\right). \tag{15}$$

Then, by combining Eq. (15) with [16, Theorem 3], the instantaneous computation rate in fading MAC with additive white Gaussian noise whose power is $\frac{1}{N}$ can be expressed as

$$R[t] = \mathsf{C}^+\left(\frac{N}{M} + N \min_{i\in[1:M]}\left[|h_{\mathcal{I}_i}[t]|^2 P_{\mathcal{I}_i}[t]\right]\right) \tag{16}$$

at the t-th time slot. Note that the symbol transmitted by a sub-carrier in OFDM lasts N time slots, whereas the symbol transmitted by the single carrier lasts one time slot. Thus, the

number of function values in a sub-carrier is $\frac{1}{N}$ of the number of function values in single carrier referred to Definition 5, which means that the computation rate of a sub-carrier is $\frac{1}{N}$ of the computation rate in Eq. (16). In conclusion, Lemma 1 has been proved. ■

C. Reconstruction of Sub-Functions

Only M nodes are chosen from all K nodes to compute a sub-function, which means there needs to be $B = \frac{K}{M}$ sub-functions to reconstruct a desired function. τ denotes a set where the elements are the indexes of the M chosen nodes for a sub-function $f\left(\{s_i[j]\}_{i\in\tau}\right)$ (see Definition 3). Then, the set

$$\mathcal{S} = \{\tau \subseteq [1:K] : |\tau| = M\} \tag{17}$$

includes all the possible sub-functions[1], and the cardinality of $\mathcal{S}$ is $|\mathcal{S}| = \binom{K}{M}$. According to Definition 3, the sub-functions can be reconstructed into the desired function if and only if $\bigcup_{u=1}^{B} \tau_u = [1:K]$, $\tau_u \bigcap \tau_v = \emptyset$ for all $u, v \in [1:B]$ and $\tau_u, \tau_v \in \mathcal{S}$. We define

$$\mathcal{Q} = \left\{ \rho = \{\tau_1, \tau_2, \cdots, \tau_B\} : \bigcup_{u=1}^{B} \tau_u = [1:K], \tau_u \in \mathcal{S} \right\}, \tag{18}$$

which contains all possible combinations that can be used to reconstruct the desired function, and $|\mathcal{Q}| = \prod_{l=0}^{B-1} \binom{K-Ml}{M}$.

Within our design, the length-n block code is transmitted through T_s OFDM symbols. In order to simplify the derivation, the number of OFDM symbols is $T_s = \frac{n}{N}$ instead of $\lceil \frac{n}{N} \rceil$ in Eq. (4), which further implies that the number of all the sub-carriers during T_s OFDM symbols is n. Based on sub-function allocation, all the sub-carriers should be assigned to a sub-function. The set $\mathcal{M}_\tau$ for all $\tau \in \mathcal{S}$ includes those sub-carriers that are assigned to sub-function τ. We let a set $\mathcal{M}_\rho^\tau$ include the sub-carriers that are from $\mathcal{M}_\tau$ and allocated to the combination $\rho \in \mathcal{Q}$ that contains the corresponding sub-function τ.

As mentioned in Issue i, Section IV-A, the order of the indexes for K nodes in each sub-carrier is random depending on channel realizations in practice. It means that the number of the sub-carriers in $\mathcal{M}_\tau$ is random. Thus, we use the following lemma to characterize the minimum deterministic values of $|\mathcal{M}_\tau|$ and $\left|\mathcal{M}_\rho^\tau\right|$.

Lemma 2: When n is large, for all $\rho \in \mathcal{Q}$ and $\tau \in \rho$, each set $\mathcal{M}_\rho^\tau$ contains

$$\left|\mathcal{M}_\rho^\tau\right| = \frac{|\mathcal{M}_\tau|}{B\frac{|\mathcal{Q}|}{|\mathcal{S}|}} = \frac{n}{B\,|\mathcal{Q}|} \tag{19}$$

sub-carriers.

Proof: The probability, $\Pr(\{\mathcal{I}_i^g[m]\}_{i=1}^M = \tau)$, for all $\tau \in \mathcal{S}$ is $\frac{1}{|\mathcal{S}|}$ since channel gains are i.i.d. in the g-th sub-carrier at the m-th OFDM symbol. Thus, $\frac{|\mathcal{M}_\tau|}{n} = \frac{1}{|\mathcal{S}|}$ holds depending on [31, Lemma 2.12]. It shows $|\mathcal{M}_\tau| = \frac{n}{|\mathcal{S}|}$ for all $\tau \in \mathcal{S}$ as n increases. Besides, in the set $\mathcal{Q}$, there are $B\frac{|\mathcal{Q}|}{|\mathcal{S}|}$ combinations which include τ as an element for all $\tau \in \mathcal{S}$. Therefore, each combination ρ including sub-function τ is assigned $\frac{|\mathcal{M}_\tau|}{B\frac{|\mathcal{Q}|}{|\mathcal{S}|}}$ sub-carriers. ■

According to the definition of $\mathcal{M}_\rho^\tau$, we find that there are $\left|\mathcal{M}_\rho^\tau\right|$ sub-carriers that are used to transmit sub-function τ in the combination ρ over T_s OFDM symbols. It also implies that the length of the transmitted signal vector of each node for sub-function $\tau \in \rho$ is $\left|\mathcal{M}_\rho^\tau\right|$. To simplify the derivation, the transmitted signal vector is sent centrally in $T_\rho = \left\lceil \frac{\left|\mathcal{M}_\rho^\tau\right|}{N} \right\rceil$ OFDM symbols. From Eq. (5), the received vector for sub-function τ based on the combination ρ at the m-th OFDM symbol in the frequency domain can be given as

$$\boldsymbol{Y}_\rho^\tau[m] = \sum_{i\in\tau} \boldsymbol{V}_{i,\rho}^\tau[m]\boldsymbol{X}_{i,\rho}^\tau[m]\boldsymbol{H}_{i,\rho}^\tau[m] + \boldsymbol{W}_\rho^\tau[m]. \tag{20}$$

Then from Eq. (5), the received signal in g-th sub-carrier can be given as

$$\begin{aligned} y_{\rho,g}^\tau[m] &= \sum_{i\in\tau} x_{i,\rho,g}^\tau[m] v_{i,\rho,g}^\tau[m] h_{i,\rho,g}^\tau[m] + w_{i,\rho,g}^\tau[m] \\ &= \sum_{i\in\tau} x_{i,\rho,g}^\tau[m] h_{i,\rho,g}^{'\tau}[m] + w_{i,\rho,g}^\tau[m], \end{aligned} \tag{21}$$

where $h_{i,\rho,g}^{'\tau}[m] = |h_{i,\rho,g}^\tau[m]|\sqrt{P_{i,\rho,g}^\tau[m]}$. From the conclusion of Lemma 1 and Eqs. (20) and (21), the average rate for computing a sub-function $f\left(\{s_i[j]\}_{i\in\tau}\right)$ during T_ρ OFDM symbols is given as

$$\begin{aligned} R_\rho &= \frac{1}{T_\rho}\sum_{m=1}^{T_\rho}\frac{1}{N}\sum_{g=1}^{N} \mathsf{C}^+\left(\frac{N}{M} + N\min_{i\in\tau}\left[|h_{i,g}[m]|^2 P_{i,g}[m]\right]\right) \\ &\overset{(a)}{=} \frac{1}{T_\rho}\sum_{m=1}^{T_\rho}\frac{1}{N}\sum_{g=1}^{N} R_{\rho,g}[m], \end{aligned} \tag{22}$$

where the condition (a) follows because $\{\mathcal{I}_i^g[m]\}_{i=1}^M = \tau$.

Note that we employ a nested lattice code in the proposed system and the length of the transmitted signal vector of each node in $\tau \in \rho$ is $\left|\mathcal{M}_\rho^\tau\right|$. In order to satisfy this length for the transmitted signal vector, the corresponding length of the data vector should be $U_\rho = \frac{R_\rho\left|\mathcal{M}_\rho^\tau\right|}{H(f(\mathbf{b_v}))}$ depending on Definition 5, which addresses Issue ii, Section IV-A. Thus, a desired function $f(\mathbf{s}[j])$ reconstructed by combination ρ can be described as $f_c(\{f(\{s_i[j]\}_{i\in\tau})\}_{\tau\in\rho})$ (see Definition 3), and the number of desired function values reconstructed by combination ρ is U_ρ. Then, the number of desired function values for all $\rho \in \mathcal{Q}$ is

$$\begin{aligned} T_d &= \sum_{\rho\in\mathcal{Q}} U_\rho \\ &= \sum_{\rho\in\mathcal{Q}} \frac{R_\rho\left|\mathcal{M}_\rho^\tau\right|}{H(f(\mathbf{b_v}))} \end{aligned} \tag{23}$$

[1]For easy presentation, we use the element $\tau \in \mathcal{S}$ stands for the sub-function $f\left(\{s_i[j]\}_{i\in\tau}\right)$ which is computed by these nodes in τ.

during T_s OFDM symbols. As a result, the computation rate based on Definition 5 for computing the desired function via CoMAC-OFDM

$$\begin{aligned} R &= \lim_{n\to\infty} \frac{T_d}{n} H(f(\mathbf{b_v})) \\ &\overset{(a)}{=} \lim_{n\to\infty} \frac{\sum\limits_{\rho\in\mathcal{Q}} \frac{R_\rho \left|\mathcal{M}_\rho^\tau\right|}{H(f(\mathbf{b_v}))}}{n} H(f(\mathbf{b_v})) \\ &\overset{(b)}{=} \lim_{n\to\infty} \frac{1}{B} \frac{1}{T_\rho \left|\rho\right| \left|\mathcal{Q}\right|} \sum_{\rho\in\mathcal{Q}} \sum_{\tau\in\rho} \sum_{m=1}^{T_\rho} \frac{1}{N} \sum_{g=1}^{N} R_{\rho,g}[m] \\ &\overset{(c)}{=} \lim_{n\to\infty} \frac{1}{BN} \frac{1}{T_s} \sum_{m=1}^{T_s} \sum_{g=1}^{N} R_{\rho,g}[m] \\ &\overset{(d)}{=} \frac{1}{BN} \mathsf{E}\left[\sum_{g=1}^{N} R_{\rho,g}\right] \end{aligned}$$

is achievable as n increases where the condition (a) follows because of Lemma 2 and Eq. (23), the condition (b) follows from Eq. (22), the cardinality of ρ is $|\rho| = B$ from Eq. (18), the condition (c) follows while $T_s = T_\rho B \left|\mathcal{Q}\right|$ and the condition (d) follows due to the increase in n. Hence, Theorem 3 has been proved.

V. Power Allocation for Sub-Function Allocation

In this section, we propose two power allocation methods to implement CoMAC-OFDM with sub-function allocation. For average power allocation, the achievable rate is given in Section V-A. We further consider an optimization problem and propose a sponge-squeezing algorithm which provides a simple and concise interpretation of the necessary optimality conditions based on the solution in Section V-B.

A. Average Power Allocation

Based on sub-function allocation discussed in Section IV-A, we propose a power allocation method with an average power constraint.

Let $P_{i,g}[m]$ represent the transmitted power in the g-th sub-carrier at the m-th OFDM symbol for the node i, which can be given as

$$P_{\mathcal{I}_i^g}[m] = \begin{cases} c\dfrac{|h_{\mathcal{I}_M^g}[m]|^2}{|h_{\mathcal{I}_i^g}[m]|^2} & i \in [1:M] \\ 0 & i \in [M+1:K] \end{cases}, \tag{24}$$

where c is a constant that needs to be determined later. Considering the average power in the g-th sub-carrier at the m-th OFDM symbol, i.e., $\mathsf{E}[x_{i,g}[m]] = \frac{P}{N}$, we have

$$\begin{aligned} \mathsf{E}[P_{i,g}[m]] &= \sum_{j=1}^{K} \Pr(i = \mathcal{I}_j^g[m]) \mathsf{E}[P_{i,g}[m] | i = \mathcal{I}_j^g[m]] \\ &= \frac{c}{K} \sum_{j=1}^{M} \mathsf{E}\left[\frac{|h_{\mathcal{I}_M^g}[m]|^2}{|h_{\mathcal{I}_i^g}[m]|^2}\right] = \frac{P}{N}. \end{aligned} \tag{25}$$

Then, we can calculate

$$c = \frac{PK}{N\sum\limits_{j=1}^{M} \mathsf{E}\left[\dfrac{|h_{\mathcal{I}_M^g}[m]|^2}{|h_{\mathcal{I}_j^g}[m]|^2}\right]} \tag{26}$$

and set

$$P_{\mathcal{I}_i^g}[m] = \begin{cases} \dfrac{KP\dfrac{|h_{\mathcal{I}_M^g}[m]|^2}{|h_{\mathcal{I}_i^g}[m]|^2}}{N\sum\limits_{j=1}^{M} \mathsf{E}\left[\dfrac{|h_{\mathcal{I}_M^g}[m]|^2}{|h_{\mathcal{I}_j^g}[m]|^2}\right]} & i \in [1:M] \\ 0 & i \in [M+1:K] \end{cases}. \tag{27}$$

We further put $P_{\mathcal{I}_i^g}[m]$ from Eq. (27) into Eq. (8) in Theorem 3, then the computation rate for CoMAC-OFDM with sub-function allocation can be written as

$$\begin{aligned} R_{C2} &= \frac{M}{KN} \mathsf{E}\left[\sum_{g=1}^{N} \mathsf{C}^+\left(\frac{N}{M} + \frac{KNP|h_{\mathcal{I}_M^g}|^2}{N\sum_{j=1}^{M} \mathsf{E}\left[\dfrac{|h_{\mathcal{I}_M^g}|^2}{|h_{\mathcal{I}_j^g}|^2}\right]}\right)\right] \\ &\overset{(a)}{=} \frac{M}{K} \mathsf{E}\left[\mathsf{C}^+\left(\frac{N}{M} + \frac{|h_{\mathcal{I}_M}|^2 KP}{M\mathsf{E}\left[\dfrac{|h_{\mathcal{I}_M}|^2}{|h|^2}\right]}\right)\right], \end{aligned} \tag{28}$$

where the condition (a) follows because the channel gains in different sub-carriers are i.i.d. random variables. In conclusion, Eq. (28) is achievable as T_s increases (see Theorem 3), which completes the proof of Corollary 2. Particularly, Corollary 1 can be proved by setting $M = K$, which means that a whole desired function is allocated to each sub-carrier.

We assume that the fusion center should have the global channel state information (CSI), whereas each node needs to know its own CSI. The following signaling procedure briefly explains how CoMAC-OFDM works with average power allocation[2].

Step 1. The fusion center broadcasts a pilot signal to all nodes, and each node calculates its own CSI at the same time.

Step 2. The fusion center collects the N channel gains from each node.

Step 3. The fusion center calculates the M-th channel gain $|h_{\mathcal{I}_M^g}[m]|^2$ in the ordered channel gains and obtains the set $\tau = \{\mathcal{I}_i^g[m]\}_{i=1}^{M}$ including the M indexes with the large channel gains at the g-th sub-carrier.

Step 4. The fusion center broadcasts $|h_{\mathcal{I}_M^g}[m]|^2$ and the ID of τ to all nodes[3] at the same time.

Step 5. The fusion center chooses a set ρ which includes the set τ and has not been broadcast for τ. If each ρ including τ has already been broadcast for τ, then a

[2]The signaling procedure is also used for the optimal power allocation in the following sub-section.

[3]With given M, K and N, assume that each $\tau \in \mathcal{S}$ and each $\rho \in \mathcal{Q}$ are recorded in the memories of each node and the fusion center at first, and each set has an ID. Thus, we only need to broadcast its ID instead of all the elements in the set.

new round begins, and it repeats the method to choose the ρ. Such a set ρ is expressed as ρ_q^r, where r stands for the r-th round and q stands for the index of the element in the set $\mathcal{Q}$.

Step 6. The fusion center broadcasts the ID of the chosen ρ_q to all nodes at the same time.

Step 7. Each node finds the set τ through the corresponding ID in its memory. Also, the set ρ_q is obtained through the corresponding ID.

Step 8. The node in the set τ is active to record the number of times when the corresponding ρ_q has already been broadcast in order to obtain the number of the rounds r. Then, ρ_q^r can be obtained in these active nodes.

Step 9. The node i in the set τ is active to transmit the signal $x_{i,\rho}^{\tau}$, which is the $[(r-1)|\mathcal{Q}|+q]$-th element in the transmitted vector $\mathbf{x}_i$ with the transmitted power through Eq. (27), where $\sum_{j=1}^{M} \mathsf{E}\left[\frac{|h_{\mathcal{I}_M^g}[m]|^2}{|h_{\mathcal{I}_j^g}[m]|^2}\right]$ is a deterministic value independent of instantaneous channel gains.

Step 10. The fusion center records the value $y_{\rho_q^r}^{\tau}$ computed by the set τ in the specific combination ρ_q^r.

Step 11. The fusion center reconstructs $y_{\rho_q^r}$ by $y_{\rho_q^r} = \sum_{\tau \in \rho_q} y_{\rho_q^r}^{\tau}$ after all parts have been received.

Step 12. The fusion center reconstructs the desired functions using the whole received vector $\mathbf{y}$.

Using this procedure, all the desired functions can be reconstructed correctly after decoding, since each $y_{\rho_q^r}$ is reconstructed correctly.

B. Optimal Power Allocation

In the above analysis, we demonstrated the computation rate of CoMAC-OFDM with average power allocation. We further find that the computation rate considering the average power constraint for each node in each sub-carrier is not optimal, since adaptive power allocation can provide a more precise control of the power. Therefore, we formulate an optimization problem and propose an algorithm called sponge-squeezing based on the solution.

1) Problem Formulation: Corollary 3 shows that the computation rate in fading MAC is the mean of the instantaneous computation rates, which means Eq. (8) can be rewritten as

$$R = \frac{1}{T_s} \sum_{m=1}^{T_s} R[m], \tag{29}$$

where the instantaneous computation rate at the m-th OFDM symbol is

$$R[m] = \frac{M}{KN} \sum_{g=1}^{N} \mathsf{C}^+ \left(\frac{N}{M} + N \min_{i \in [1:M]} \left[|h_{\mathcal{I}_i^g}[m]|^2 P_{\mathcal{I}_i^g}[m] \right] \right). \tag{30}$$

This implies that our power allocation should focus on the current OFDM symbol depending on the channel gains of each sub-carrier. Thus, the optimization problem with sub-function allocation is given as

$$\begin{aligned} \underset{P_{\mathcal{I}_i^g}[m]}{\text{maximize}} \quad & R[m] \\ \text{s.t.} \quad & \sum_{g=1}^{N} P_{i,g}[m] \le P \quad \forall i \in [1:K]. \end{aligned} \tag{31}$$

From Eq. (30), we find that the problem is difficult to solve, because the $\min$ function is nested inside the $\log$ function in the objective function, and the ordered indexes $\{\mathcal{I}_i^g[m]\}_{i \in [1:M]}$ also bring difficulty. In order to make it tractable, we introduce a $K \times N$ sub-function allocation matrix $\boldsymbol{\omega}$, and each element is given as

$$\omega_{\mathcal{I}_i^g, g}[m] = \begin{cases} 1 & i \in [1:M] \\ 0 & i \in [M+1:K] \end{cases} \quad \forall g \in [1:N]. \tag{32}$$

Furthermore, $\min_{i \in [1:M]} \left[|h_{\mathcal{I}_i^g}[m]|^2 P_{\mathcal{I}_i^g}[m] \right]$ in Eq. (30) implies that the computation rate is only determined by the node with the minimum product among the M chosen nodes in the g-th sub-carrier. This means that other nodes do not need to put much power to this sub-carrier except for the node with the minimum product, and the unused power can be allocated to other sub-carriers to improve the rate. Thus, we use the level $\eta_g[m]$ to replace the $\min$ function by making $|h_{\mathcal{I}_i^g}[m]|^2 P_{\mathcal{I}_i^g}[m] = \eta_g[m]$ for all $i \in [1:M]$ in the g-th sub-carrier. Then, the optimization objective can be written as

$$R_{C3}[m] = \frac{M}{KN} \sum_{g=1}^{N} \mathsf{C}^+ \left(\frac{N}{M} + N \eta_g[m] \right). \tag{33}$$

Therefore, the problem can be expressed as:

$$\begin{aligned} \underset{\eta_g[m]}{\text{maximize}} \quad & R_{C3}[m] \\ \text{s.t.} \quad & \sum_{g=1}^{N} G_{i,g}[m] \eta_g[m] \omega_{i,g}[m] \le P \quad \forall i \in [1:K], \end{aligned} \tag{34}$$

where $\eta_g[m] \ge 0$ and $P_{i,g}[m] \ge 0$ are necessary, $G_{i,g}[m] = 1/|h_{i,g}[m]|^2$, $P_{i,g}[m] = G_{i,g}[m]\eta_g[m]$ and $\omega_{i,g}[m]$ is the element of the sub-function allocation matrix in the m-th OFDM symbol.

Note that the objective function in Eq. (34) is concave since it is a sum of $\log$ functions, which are concave themselves. Besides, the constraint set is convex as it is composed of linear constraints. Hence, the above optimization problem is a convex optimization problem, and has a unique maximum. The Lagrangian function

$$\begin{aligned} \mathcal{L} = & \frac{M}{KN} \sum_{g=1}^{N} \mathsf{C}^+ \left(\frac{N}{M} + N \eta_g[m] \right) \\ & - \sum_{i=1}^{K} \mu_i \left(\sum_{g=1}^{N} G_{i,g}[m] \eta_g[m] \omega_{i,g}[m] - P \right) \end{aligned} \tag{35}$$

with the complimentary slackness condition

$$\mu_i \left(\sum_{g=1}^{N} G_{i,g}[m]\eta_g[m]\omega_{i,g}[m] - P \right) = 0 \quad \forall i \in [1:K] \tag{36}$$

is given, where $\{\mu_i\}$ are Lagrange multipliers.

We apply the KKT optimality conditions to the Lagrangian function to obtain the optimal level $\eta_g^*[m]$ for all $g \in [1:N]$ in terms of the Lagrange multipliers $\{\mu_i\}_{i=1}^K$. Then, the optimal level $\eta_g^*[m]$ is expressed as

$$\eta_g^*[m] = \max\left\{0, v_g - \frac{1}{M}\right\}, \tag{37}$$

where

$$v_g = \frac{M}{KN\sum_{i=1}^{K}\mu_i G_{i,g}[m]\omega_{i,g}[m]}, \tag{38}$$

while $\eta_g^*[m]$ satisfies

$$\max_{i=1}^{K}\left[\sum_{g=1}^{N} G_{i,g}[m]\eta_g[m]\omega_{i,g}[m]\right] - P = 0. \tag{39}$$

Note that the optimal level $\eta_g^*[m]$ is determined by the dot product of the Lagrange multiplier vector and the channel gain vector, which is different from a family of water-filing solutions [32] determined by the single Lagrange multiplier or the sum of the Lagrange multiplier vector.

Eqs. (37) and (39) also imply that the optimal power in each sub-carrier for each node is

$$P_{i,g}^*[m] = G_{i,g}[m]\eta_g^*[m]\omega_{i,g}[m]. \tag{40}$$

In conclusion, Corollary 3 holds.

The signaling procedure for optimal power allocation is similar to the procedure for average power allocation in Section V-A. The difference is that the fusion center, considering optimal power allocation, needs to broadcast the optimal level $\eta_g^*[m]$ to all nodes at the same time.

2) Sponge-Squeezing: According to the optimal solution proposed in Eqs. (37), (38) and (40), the solution is quite different from the solution of the conventional power allocation with OFDM [32], since the solution to our problem is determined by the dot product of the Lagrange multiplier vector and the channel gain vector, whereas a family of water-filing solutions [32] are determined by the single Lagrange multiplier or the sum of the Lagrange multiplier vector. This means that the classical water-filling algorithm cannot be used to solve this problem. Even if the above optimization problem, i.e., a convex optimization problem, is solved by some math-tools such as CVX and MATLAB through gradient descent or interior point method, the performance of such method decreases rapidly as the number of sub-carriers N and the number of nodes K increase. Thus, we propose an algorithm called sponge-squeezing based on the KKT optimality conditions, which can achieve the same accuracy as CVX and improve the performance.

The principle of the algorithm, sponge-squeezing, can be summarized as follows. For any node i, it owns N sponges which stand for N sub-carriers. And the volume of water that a node owns is P, which stands for the power of the node

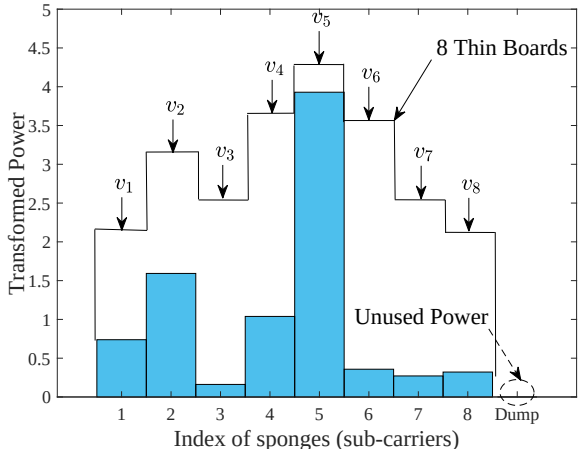

(a) Initialization phase

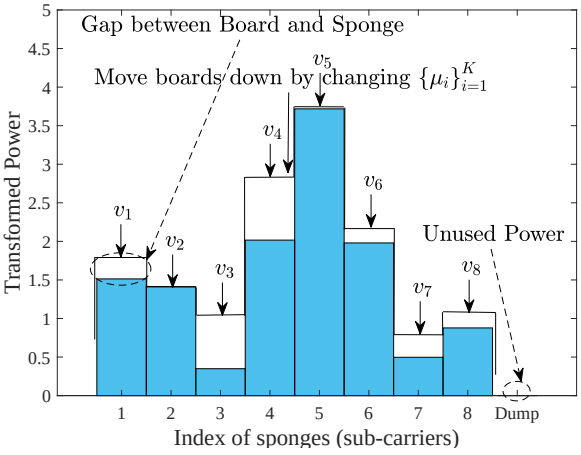

(b) Squeezing phase

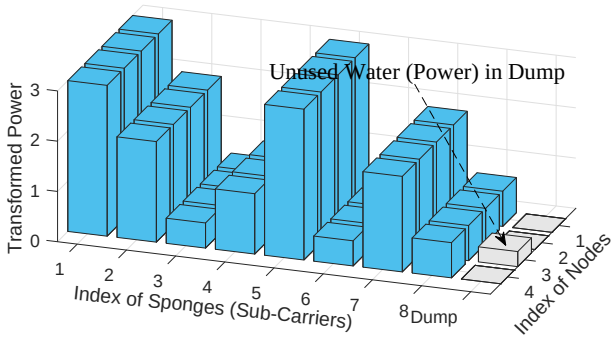

(c) Termination phase

Fig. 3. Schematic diagram for sponge-squeezing

i. Each sponge can swell and become higher after absorbing water. Moreover, different sponges have different swell factors depending on $\frac{1}{G_{i,g}[m]\omega_{i,g}[m]}$ (see Eq. (40)) for the node i in the g-th sponge. Then, put these sponges into the container i.

Initialization phase. Node i pours water into the container, and each sponge can evenly absorb water of which the volume is $\frac{P}{N}$. Because of the different swell factors, each sponge reaches different height after absorbing water. We place N thin boards above these containers and the height of the g-th thin board depends on v_g (see Eq. (38)). As shown in Fig. 3a, a node has 8 sponges, and different sponges reach different heights after absorbing the same volume of water. Meanwhile, there are 8 thin boards over these sponges with different heights.

Squeezing phase. We change the value of these Lagrange multipliers $\{\mu_i\}_{i=1}^{K}$, and all these thin boards start to fall and reach new heights. Note that some boards may fall fast and others fall slow due to v_g. When a thin board presses on the sponge, some water in this sponge is squeezed out and is absorbed by other sponges in this container. And the lower the thin board is, the more water the sponge squeezes out. If all these sponges are pressed under these boards, the unused water is put into the dump.

Termination phase. We move these boards down until there is no gap between these boards and every sponge for every node while at least one dump is empty to satisfy Eq. (39). The result with 4 nodes is shown in Fig. 3c.

VI. Simulation Results and Discussions

In this section, we provide some simulation results of the computation rate under sub-function allocation based on CoMAC-OFDM and compare it with these CoMAC-SC schemes. In our simulation, the average signal-to-noise ratio (SNR) is the same as P because the variance of the noise is set to one. We consider i.i.d. Rayleigh fading channel, i.e., the exponential distribution with parameter one, in each sub-carrier and each OFDM symbol. For easy presentation, the abbreviation for sub-function allocation, average power allocation and optimal power allocation are SFA, APA and OPA, respectively.

The rate of CoMAC-OFDM with SFA and APA in Corollary 2 with respect to M and N is shown in Fig. 4. Under sub-function allocation, M nodes participate in the computation of a sub-function. As the number of sub-carriers N increases, the computation rate increases. Due to the optimal power allocation, the rate of CoMAC-OFDM with SFA and OPA always outperforms others. By setting $N = 1$ for CoMAC-OFDM with SFA and APA, the rate of opportunistic CoMAC-SC in Theorem 2 is a special case. Furthermore, this shows that there is an optimal M to achieve the largest computation rate with a fixed N, which also means that the computation rate is determined by the number of sub-functions $B = \frac{K}{M}$.

Since the number of sub-functions B determines the computation rate, it is necessary to find the optimal B. In Fig. 5, the relationship between the number of nodes K and the number of sub-functions B is given. When K is small, we find that there is no need to divide the desired function into several

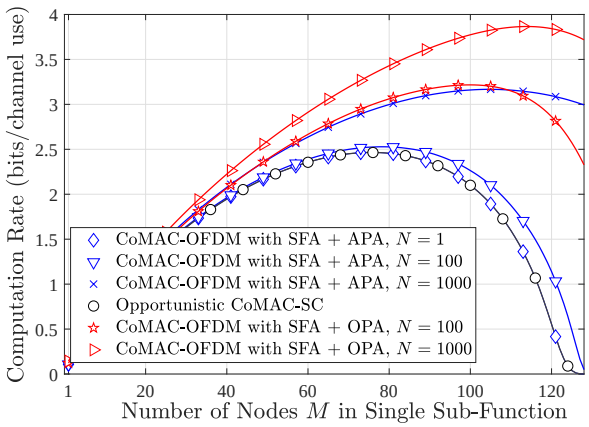

Fig. 4. Computation rates with respect to M and N when $K = 128, P = 10$ dB.

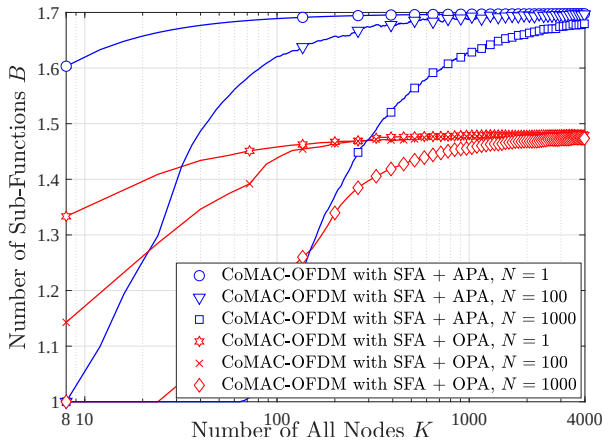

Fig. 5. Optimal number of sub-functions with respect to K and N when $P = 10$ dB.

sub-functions. However, for a large K (i.e, 4000), the number of sub-functions B increases and converges to 2 because B belongs to $\mathbb{N}$. The result demonstrates that sub-function allocation is necessary to approach the largest computation rate. Furthermore, with the same P, CoMAC-OFDM with SFA and OPA can use fewer sub-functions since the optimal power allocation provides a more precise way to allocate power to each node. Due to the reconstruction with fewer sub-functions, CoMAC-OFDM with SFA and OPA can provide an improved performance compared with CoMAC-OFDM with SFA and APA.

In addition, considering average power allocation, we compare CoMAC-OFDM with CoMAC-SC. As shown in Fig. 6, the rate of direct CoMAC-SC is the worst one and converges to 0 rapidly as K increases. The rate of direct CoMAC-OFDM is improved as N increases compared with the rate of direct CoMAC-SC. However, it still cannot avoid a vanishing computation rate as K increases. Moreover, the result shows that CoMAC-OFDM with SFA and APA can provide a non-vanishing computation rate like opportunistic CoMAC-SC as K increases, but CoMAC-OFDM with SFA and APA can

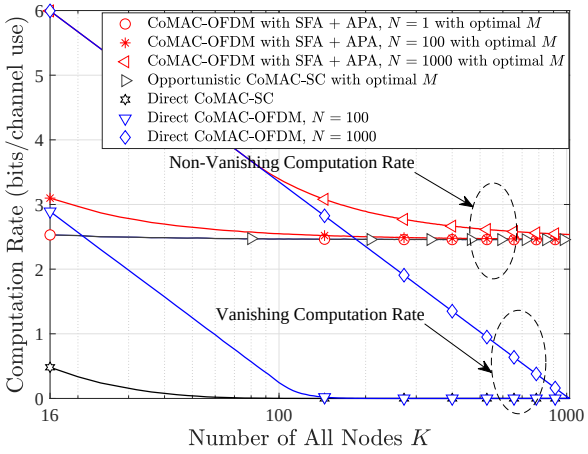

Fig. 6. Comparison between CoMAC-OFDM and CoMAC-SC when $P = 10$ dB.

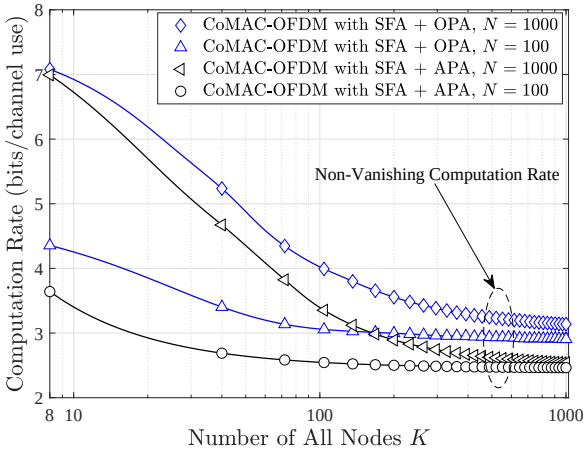

Fig. 7. Comparison between optimal power allocation and average power allocation in CoMAC-OFDM with sub-function allocation when $P = 10$ dB.

achieve a higher computation rate as N increases. Furthermore, opportunistic CoMAC-SC is a special case by setting $N = 1$ in CoMAC-OFDM with SFA and APA.

In Fig. 7, CoMAC-OFDM with SFA and OPA provides a higher rate than CoMAC-OFDM with SFA and APA. It shows that the computation rate can be further improved by optimal power allocation and also provide a non-vanishing computation rate as K increases.

Finally, the complexity of the proposed optimal power allocation versus the average power allocation is shown in Fig. 8. For CoMAC-OFDM with SFA and OPA, we compare our sponge-squeezing algorithm with CVX. By setting the same accuracy, i.e., 10^{-4} as the stopping criterion for the iterations, we ran both algorithms on a desktop with 2.40-GHz CPU. This shows that the sponge-squeezing algorithm has a faster speed than CVX. When the number of sub-carriers increases, the advantage of the sponge-squeezing algorithm becomes more obvious. Since we provide a closed-form expression, i.e., Eq. (27), for CoMAC-OFDM with SFA and APA, the complexity of it is very small, and most of the time that it takes is to sort the channel gains in each sub-carrier.

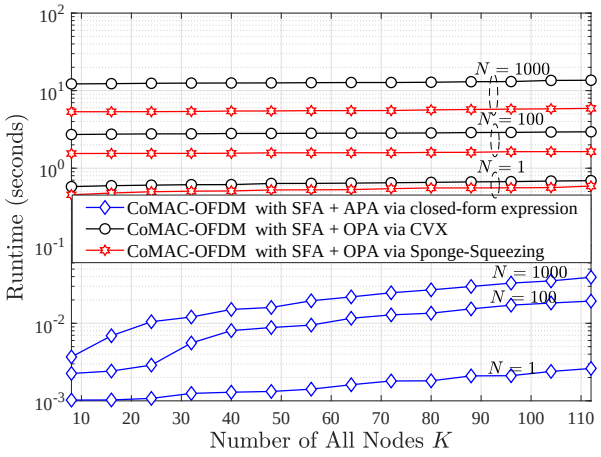

Fig. 8. Complexity of the optimal power allocation versus the average power allocation.

VII. Conclusion

In this paper, we have studied CoMAC for wide-band transmission, and focused on designing a framework of CoMAC that can combat frequency-selective fading and vanishing computation rate. To tackle these problems, we have utilized OFDM in CoMAC. CoMAC-OFDM cannot execute conventional bit allocation in different sub-carriers, because it aims at transmitting a desired function over the air instead of bit sequences. Hence, a novel sub-function allocation has been proposed to handle this issue through the division, allocation and reconstruction of functions. The theoretical expression of achievable computation rate has been derived based on the classical results of nested lattice coding, which provides a non-vanishing computation rate as the number of nodes increases. Furthermore, we have discussed an optimization problem, and a sponge-squeezing algorithm extended from the classical water-filling algorithm is proposed to carry out the optimal power allocation method. The results have showed that the computation rate can be improved by optimal power allocation, and a non-vanishing computation rate is also provided as K increases.

Acknowledgment

The authors would like to thank Dr. Adam Noel for his advice and proofreading of our manuscript.

References

[1] G. Fettweis and S. Alamouti, "5G: Personal mobile internet beyond what cellular did to telephony," *IEEE Commun. Mag.*, vol. 52, no. 2, pp. 140–145, 2014.

[2] A. Al-Fuqaha, M. Guizani, M. Mohammadi, M. Aledhari, and M. Ayyash, "Internet of things: A survey on enabling technologies, protocols, and applications," *IEEE Commun. Surv. Tutorials*, vol. 17, no. 4, pp. 2347–2376, 2015.

[3] A. Gupta and R. K. Jha, "A survey of 5G network: Architecture and emerging technologies," *IEEE access*, vol. 3, pp. 1206–1232, 2015.

[4] M. Goldenbaum, H. Boche, and S. Stańczak, "Nomographic functions: Efficient computation in clustered Gaussian sensor networks," *IEEE Trans. Wireless Commun.*, vol. 14, no. 4, pp. 2093–2105, 2015.

[5] M. Goldenbaum and S. Stanczak, "Robust analog function computation via wireless multiple-access channels," *IEEE Trans. Commun.*, vol. 61, no. 9, pp. 3863–3877, 2013.

[6] O. Abari, H. Rahul, and D. Katabi, "Over-the-air function computation in sensor networks," *arXiv preprint arXiv:1612.02307*, 2016.

[7] M. Goldenbaum and S. Stanczak, "On the channel estimation effort for analog computation over wireless multiple-access channels," *IEEE Wireless Commun. Lett.*, vol. 3, no. 3, pp. 261–264, 2014.

[8] A. Kortke, M. Goldenbaum, and S. Stańczak, "Analog computation over the wireless channel: A proof of concept," in *SENSORS, 2014 IEEE*. IEEE, 2014, pp. 1224–1227.

[9] G. Zhu, L. Chen, and K. Huang, "Over-the-air computation in MIMO multi-access channels: Beamforming and channel feedback," *arXiv preprint arXiv:1803.11129*, 2018.

[10] L. Chen, N. Zhao, Y. Chen, F. R. Yu, and G. Wei, "Over-the-air computation for IoT networks: Computing multiple functions with antenna arrays," *IEEE IoT J.*, vol. 5, no. 6, pp. 5296–5306, 2018.

[11] B. Nazer and M. Gastpar, "Computation over multiple-access channels," *IEEE Trans. Inf. Theory*, vol. 53, no. 10, pp. 3498–3516, 2007.

[12] R. Appuswamy and M. Franceschetti, "Computing linear functions by linear coding over networks," *IEEE Trans. Inf. Theory*, vol. 60, no. 1, pp. 422–431, 2014.

[13] U. Erez, S. Litsyn, and R. Zamir, "Lattices which are good for (almost) everything," *IEEE Trans. Inf. Theory*, vol. 51, no. 10, pp. 3401–3416, 2005.

[14] L. Chen, X. Qin, and G. Wei, "A uniform-forcing transceiver design for over-the-air function computation," *IEEE Wireless Commun. Lett.*, vol. 7, no. 6, pp. 942–945, 2018.

[15] B. Nazer and M. Gastpar, "Compute-and-forward: Harnessing interference through structured codes," *IEEE Trans. Inf. Theory*, vol. 57, no. 10, pp. 6463–6486, 2011.

[16] S.-W. Jeon, C.-Y. Wang, and M. Gastpar, "Computation over Gaussian networks with orthogonal components," *IEEE Trans. Inf. Theory*, vol. 60, no. 12, pp. 7841–7861, 2014.

[17] S. W. Jeon and C. J. Bang, "Opportunistic function computation for wireless sensor networks," *IEEE Trans. Wireless Commun.*, vol. 15, no. 6, pp. 4045–4059, 2016.

[18] C.-Y. Wang, S.-W. Jeon, and M. Gastpar, "Interactive computation of type-threshold functions in collocated Gaussian networks," *IEEE Trans. Inf. Theory*, vol. 61, no. 9, pp. 4765–4775, 2015.

[19] M. Goldenbaum, "Computation of real-valued functions over the channel in wireless sensor networks," Ph.D. dissertation, Technische Universität München, 2014.

[20] D. Tse and P. Viswanath, *Fundamentals of wireless communication*. Cambridge university press, 2005.

[21] Z. Hasan, G. Bansal, E. Hossain, and V. K. Bhargava, "Energy-efficient power allocation in OFDM-based cognitive radio systems: A risk-return model," *IEEE Trans. Wireless Commun.*, vol. 8, no. 12, 2009.

[22] C. Mohanram and S. Bhashyam, "Joint subcarrier and power allocation in channel-aware queue-aware scheduling for multiuser OFDM," *IEEE Trans. Wireless Commun.*, vol. 6, no. 9, 2007.

[23] Y.-F. Chen and J.-W. Chen, "A fast subcarrier, bit, and power allocation algorithm for multiuser OFDM-based systems," *IEEE Trans. Veh. Technol.*, vol. 57, no. 2, pp. 873–881, 2008.

[24] T. Berger, Z. Zhang, and H. Viswanathan, "The CEO problem [multiterminal source coding]," *IEEE Trans. Inf. Theory*, vol. 42, no. 3, pp. 887–902, 1996.

[25] T. A. Courtade and T. Weissman, "Multiterminal source coding under logarithmic loss," *IEEE Trans. Inf. Theory*, vol. 60, no. 1, pp. 740–761, 2014.

[26] Y. Ugur, I. E. Aguerri, and A. Zaidi, "Vector Gaussian CEO problem under logarithmic loss and applications," *arXiv preprint arXiv:1811.03933*, 2018.

[27] I. E. Aguerri, A. Zaidi, G. Caire, and S. S. Shitz, "On the capacity of cloud radio access networks with oblivious relaying," in *2017 IEEE International Symposium on Information Theory (ISIT)*. IEEE, 2017, pp. 2068–2072.

[28] A. Giridhar and P. R. Kumar, "Computing and communicating functions over sensor networks," *IEEE J. Sel. Areas Commun.*, vol. 23, no. 4, pp. 755–764, 2005.

[29] J. Zhan, S. Y. Park, M. Gastpar, and A. Sahai, "Linear function computation in networks: Duality and constant gap results," *IEEE J. Sel. Areas Commun.*, vol. 31, no. 4, pp. 620–638, 2013.

[30] N. Ma, P. Ishwar, and P. Gupta, "Interactive source coding for function computation in collocated networks," *IEEE Trans. Inf. Theory*, vol. 58, no. 7, pp. 4289–4305, 2012.

[31] I. Csiszar and J. Körner, *Information Theory: Coding Theorems for Discrete Memoryless Systems*. Cambridge University Press, 2011.

[32] D. P. Palomar and J. R. Fonollosa, "Practical algorithms for a family of waterfilling solutions," *IEEE Trans. Signal Process.*, vol. 53, no. 2, pp. 686–695, 2005.

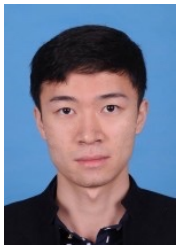

Fangzhou Wu received the B.S. degree in electronic information engineering from North China Electric Power University, Beijing, China, in 2016. He is currently pursuing the Ph.D. degree with the Department of Electronic Engineering and Information Science, CAS Key Laboratory of Wireless-Optical Communications, University of Science and Technology of China. His research interests include visible light communications, and wireless communication and computation.

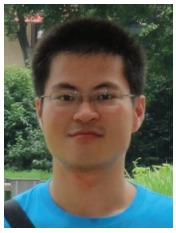

Li Chen received the B.E. in electrical and information engineering from Harbin Institute of Technology, Harbin, China, in 2009 and the Ph.D. degree in electrical engineering from the University of Science and Technology of China, Hefei, China, in 2014. He is currently an Associate Professor with the Department of Electronic Engineering and Information Science, University of Science and Technology of China. His research interests include wireless IoT communications and wireless optical communications.

Nan Zhao (S'08-M'11-SM'16) is currently an Associate Professor at Dalian University of Technology, China. He received the Ph.D. degree in information and communication engineering in 2011, from Harbin Institute of Technology, Harbin, China.

Dr. Zhao is serving or served on the editorial boards of 7 SCI-indexed journals, including IEEE Transactions on Green Communications and Networking. He won the best paper awards in IEEE VTC 2017 Spring, MLICOM 2017, ICNC 2018, WCSP 2018 and CSPS 2018. He also received the IEEE Communications Society Asia Pacific Board Outstanding Young Researcher Award in 2018.

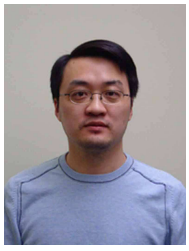

Yunfei Chen (S'02-M'06-SM'10) received his B.E. and M.E. degrees in electronics engineering from Shanghai Jiaotong University, Shanghai, P.R.China, in 1998 and 2001, respectively. He received his Ph.D. degree from the University of Alberta in 2006. He is currently working as an Associate Professor at the University of Warwick, U.K. His research interests include wireless communications, cognitive radios, wireless relaying and energy harvesting.

F. Richard Yu (S'00-M'04-SM'08-F'18) received the PhD degree in electrical engineering from the University of British Columbia (UBC) in 2003. From 2002 to 2006, he was with Ericsson (in Lund, Sweden) and a start-up in California, USA. He joined Carleton University in 2007, where he is currently a Professor. He received the IEEE Outstanding Service Award in 2016, IEEE Outstanding Leadership Award in 2013, Carleton Research Achievement Award in 2012, the Ontario Early Researcher Award (formerly Premiers Research Excellence Award) in 2011, the Excellent Contribution Award at IEEE/IFIP TrustCom 2010, the Leadership Opportunity Fund Award from Canada Foundation of Innovation in 2009 and the Best Paper Awards at IEEE ICNC 2018, VTC 2017 Spring, ICC 2014, Globecom 2012, IEEE/IFIP TrustCom 2009 and Int'l Conference on Networking 2005. His research interests include wireless cyber-physical systems, connected/autonomous vehicles, security, distributed ledger technology, and deep learning.

He serves on the editorial boards of several journals, including Co-Editor-in-Chief for Ad Hoc & Sensor Wireless Networks, Lead Series Editor for IEEE Transactions on Vehicular Technology, IEEE Transactions on Green Communications and Networking, and IEEE Communications Surveys & Tutorials. He has served as the Technical Program Committee (TPC) Co-Chair of numerous conferences. Dr. Yu is a registered Professional Engineer in the province of Ontario, Canada, a Fellow of the Institution of Engineering and Technology (IET), and a Fellow of the IEEE. He is a Distinguished Lecturer, the Vice President (Membership), and an elected member of the Board of Governors (BoG) of the IEEE Vehicular Technology Society.

Guo Wei received the B.S. degree in electronic engineering from the University of Science and Technology of China (USTC), Hefei, China, in 1983 and the M.S. and Ph.D. degrees in electronic engineering from the Chinese Academy of Sciences, Beijing, China, in 1986 and 1991, respectively. He is currently a Professor with the School of Information Science and Technology, USTC. His current research interests include wireless and mobile communications, wireless multimedia communications, and wireless information networks.